ORGANIC CHEMISTRY FRONTIERS

RESEARCH ARTICLE

View Article Online
View Journal | View Issue

Cite this: *Org. Chem. Front.*, 2023, **10**, 1915

Synthesis of α-amino acid derived (1,2,3-triazol-4-yl)-picolinamide (tzpa) ligands and their corresponding luminescent Tb(III) complexes†

Isabel N. Hegarty,[a] Chris S. Hawes [b] and Thorfinnur Gunnlaugsson *[a]

Received 14th February 2023,
Accepted 8th March 2023

DOI: 10.1039/d3qo00232b

rsc.li/frontiers-organic

The synthesis of chiral α-amino acid derived (1,2,3-triazol-4-yl)-picolinamide (**tzpa**) ligands **4–6** designed by combining the coordination properties of two well-known ligand structures within a single unit is described. The self-assembly formation between these ligands and the lanthanide ion Tb(III) was investigated in solution by probing the ground and the singlet excited state properties of the ligands as well as monitoring the evolution of the Tb(III) emission at long wavelengths. The spectroscopic results showed that while under thermodynamic control the 1 : 3 (Tb : L) is produced, then analysis of the titration data using non-liner regression analysis demonstrated that the main species in solution is the 1 : 2 (Tb : L) after the addition of 0.5 equivalents of Tb(III).

The formation of chiral ligands for use in metal directed synthesis of coordination complexes[1] and supramolecular self-assemblies[2,3] has become a highly active area of research in recent times.[4] This development has led to the synthesis of a wide range of organic ligands,[5,6] which in conjunction with either d- or f-metal ions[7–9] can result in the formation of both structurally versatile and beautiful structures,[10] the synthesis of which cannot be achieved without the use of such a template synthesis.[11,12] Furthermore, the physical properties of the ions themselves can be transferred to such structures, often resulting in the generation of systems possessing novel structural, physical and material properties.[13,14] We have developed many examples of such chiral organic ligands and chiral metal templated self-assemblies in the past.[15–18] In particular, we have probed their structural properties, as well as their physical organic and material properties in both solution and the solid state.[19] We recently developed a new family of ligands based on the (1,2,3-triazol-4-yl)-picolinamide (**tzpa**) core, as depicted schematically in Fig. 1.[20,21] The **tzpa** family are designed by combining two effective ligand motifs, namely 2,3-bis(1,2,3-triazol-4-yl)picolinamide (**btp**) and dipicolinic acid/amide (**dpa**), both of which we have synthesized and employed in our studies over the years.[22,23] Here, we present the synthesis of two chiral **tzpa** ligands (shown as **4** and **5** in Scheme 1) from L-amino acids (as protected esters), and investigate their interactions with the lanthanide ion Tb(III) by probing their ground and excited state properties in solution. The lanthanides have high coordination requirements which can be fulfilled with such tridentate ligands.[24] As depicted in Fig. 1, the formation of the 1 : 3 (M : L) stoichiometry would give rise to a fully saturated coordination environment, where each ligand coordinates with the Ln(III) ion *via* the pyridine nitrogen, as well as the carboxylic unit, and the triazole moiety. However, other stoichiometries can also exist which can be determined by carrying out spectroscopic titration studies and fitting the resulting data using non-linear regression analysis. Here, we give a full account of our investigation for ester ligands **4** and **5** as well as the carboxylic acid derivative **6**, formed from **4**. We also show that in the presence of the lanthanide ion Tb(III), the ligands form luminescent complexes both under thermodynamic and kinetic conditions.

Fig. 1 Graphical representation of the (1,2,3-triazol-4-yl)-picolinamide (**tzpa**) core (X = phenyl, amino acid derived phenyl linker, *etc.*; Y = H, ester, amide, *etc.*), and the formation of the 1 : 3 (M : L) complex with lanthanide (Ln) salts. Such complexes (*e.g.* using ligands **4** and **5** developed herein) can be formed either under thermodynamic or kinetic control.

[a]*School of Chemistry and Trinity Biomedical Science Institute, University of Dublin, Trinity College Dublin, Dublin 2, Ireland. E-mail: gunnlaut@tcd.ie*
[b]*School of Chemical and Physical Sciences, Keele University, Keele ST5 5BG, UK*

† Electronic supplementary information (ESI) available: Additional spectroscopic data and crystallographic data table. CCDC 2239920. For ESI and crystallographic data in CIF or other electronic format see DOI: **https://doi.org/10.1039/d3qo00232b**

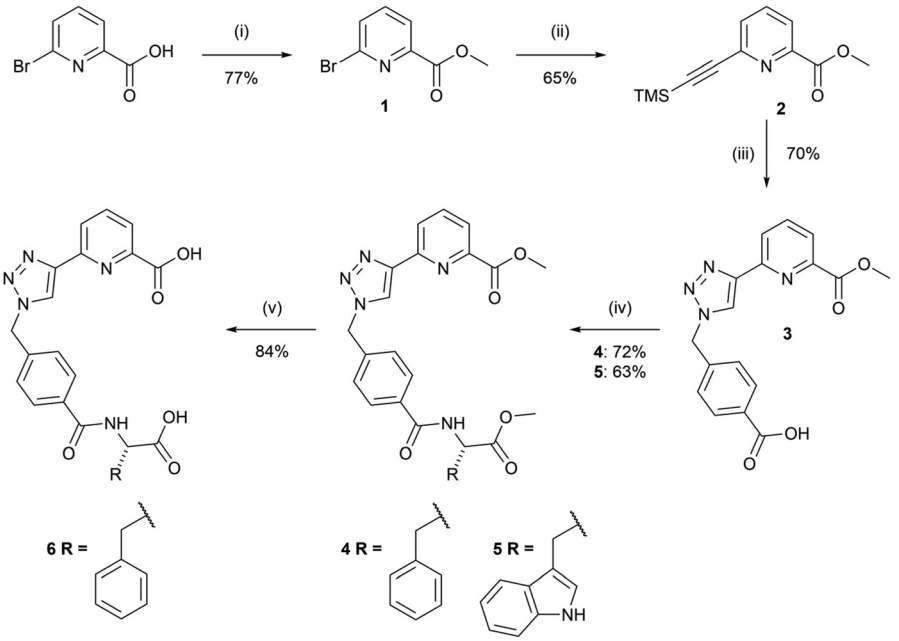

Scheme 1 The structure and synthesis of compounds **1–6**. Reagents and conditions: (i) CH_3OH, H_2SO_4, (ii) ethynyltrimethylsilane, THF:NEt_3, $Pd(PPh_3)_4$, CuI (iii) NaN_3, $CuSO_4{\cdot}5H_2O$, 4-(bromomethyl)benzoic acid, sodium ascorbate, K_2CO_3, DMF/H_2O (iv) **4** : L-phenylalanine HCl **5**: L-trpytophan HCl, HOBt, DMF/CH_2Cl_2, NEt_3, and EDC·HCl. (vi) NaOH, 100 °C.

Results and discussion

Synthesis and characterisation of ligands 4–6 and the Tb(III) complexes of 4 and 5

The syntheses of the chiral **tzpa**-derived ligands **4** and **5** from (*S*) phenylalanine or tryptophan methyl esters were undertaken (Scheme 1). These amino acids were chosen as they are known to be able to populate the Tb(III) excited state through sensitisation, or the so-called antenna effect.[25] Having developed **btp** based amino acid derived structures in the past with the view of making 'peptide bundles',[26] our initial objective was to synthesise the methyl ester-protected ligands, which could then be hydrolysed and further synthetically modified. In that work we also showed that the Tb(III) complexes are significantly more emissive than their corresponding Eu(III) complexes. Although we did study in part the interaction of **4** with Eu(III), the focus herein is on Tb(III) systems.

The route to **4** and **5** included four steps starting with the formation of methyl-6-bromopicolinate, **1**, from 6-bromopyridine-2-carboxylic acid in the presence of sulfuric acid and CH_3OH under reflux conditions. This compound was then subjected to Sonogashira coupling with ethynyltrimethylsilane in a THF/NEt_3 mixture using $Pd(PPh_3)_4$ as a catalyst. The crude product **2** was isolated as a brown oil, and purified using column chromatography to give **2** as a brown solid in 65% yield. 4-(Bromomethyl)benzoic acid was then converted to the relevant azide using sodium azide and employed in a CuAAC reaction *in situ* with compound **2** to generate compound **3**. **3** was isolated by initial washing with an EDTA solution in aqueous ammonia, followed by acidification using 1M HCl which resulted in the precipitation of the desired product as a white solid in 70% yield. Compound **3** was then reacted with L-phenylalanine methyl ester hydrochloride or L-tryptophan methyl ester hydrochloride in a peptide coupling reaction to generate compounds **4** and **5** as white solids in yields of 72% and 63%, respectively.

Compound **4** could also be hydrolysed with 1M NaOH under reflux conditions overnight. As Ln(III) coordination would be around the **tzpa** pocket and not involve the terminal amino acid moiety, this provides a handle for further modification, for instance in the generation of soft materials, where the acid unit is employed to extend the overall supramolecular assembly. This we have demonstrated for both **btp** and **dpa** ligands in the past, which in the presence of Ln(III) ions formed soft materials.[27] With this in mind, we hydrolysed the ester of **4** to give **6** in a 1M NaOH solution under reflux for 3 hours. Upon cooling and subsequent addition of 1M HCl, compound **6** precipitated out of solution as a pure white solid.

All compounds discussed above were characterised by NMR spectroscopy, HRMS and IR spectroscopy (see select examples in the ESI†). The ^{1}H NMR spectra of compounds **4** and **5** are shown in Fig. 2 (see the ESI† for their ^{13}C NMR spectra). The resonance corresponding to the pyridyl protons of both ligands reside at 8.26, 8.10 and 8.01 ppm while the triazole protons lie downfield at 8.81 ppm. The aromatic protons H_a and H_b resonate at 7.82 and 7.47 ppm as two doublets and the adjacent CH_2 protons are located at 5.75 ppm in both compounds. The multiplet upfield at 4.65 ppm corresponds to the proton H_c while the methyl protons associated with the pyridyl ring and the amino acid moiety lie at 3.91 and 3.62 ppm,

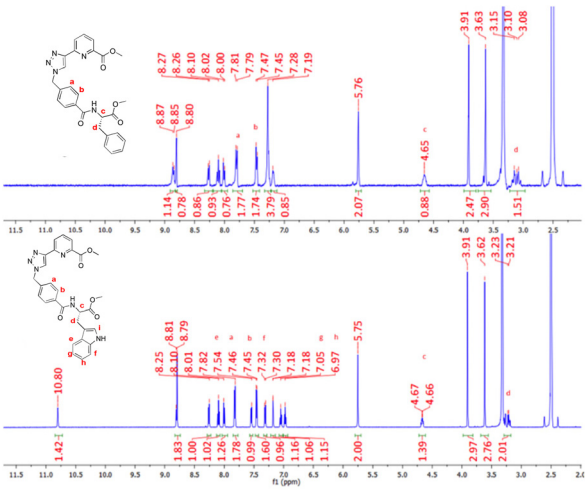

Fig. 2 The ^{1}H NMR spectra (600 MHz, DMSO-d_6) of (top) compounds **4** and (bottom) **5**.

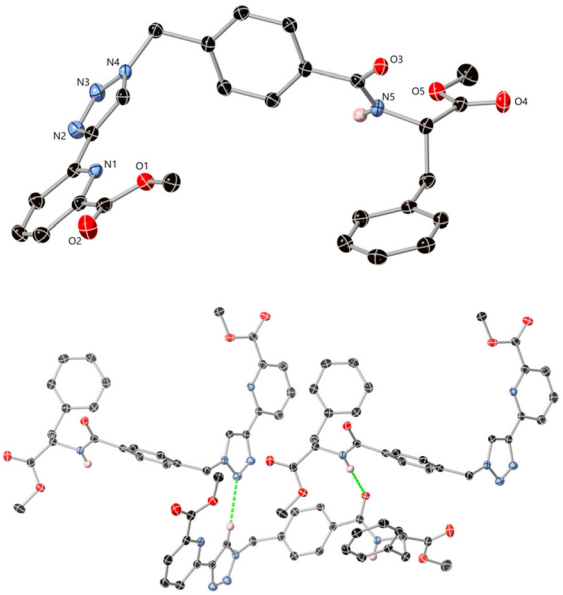

Fig. 3 (Top) Structure of one unique molecule of compound **4** with heteroatom labelling scheme. Selected hydrogen atoms are omitted for clarity. (Bottom) Primary modes of interaction between two molecules. Selected hydrogen atoms are omitted for clarity. ADPs are provided at the 50% probability level.

respectively. Finally, the protons at 3.1–3.2 ppm were assigned to the CH_2 protons H_d. In the case of **4**, the phenylalanine residue generates resonances at 7.28 and 7.19 ppm which correspond to the phenyl ring of the appended amino acid, integrating to five protons overall. Similarly, for compound **5** the doublet signals located at 7.54 and 7.31 ppm correspond to the tryptophan protons H_e and H_f while the triplets at 7.05 and 6.97 ppm can be assigned to protons H_g and H_h. The proton H_i resonates at 7.18 ppm while the amide proton of the tryptophan moiety was located downfield at 10.8 ppm. Both ligands **4** and **5** have chiral chromophores as part of their structures, and consequently, their CD spectra were recorded. Unfortunately, in both cases, these (appearing at high energy) were both very weak and poorly resolved.

In addition to the above charactersation, single crystals of compound **4** of X-ray diffraction quality were obtained by evaporation of a solution of **4** from CH_3OH, which was analysed in the monoclinic space group $P2_1$. The asymmetric unit contains one molecule of the ligand, Fig. 3 (see further information in the ESI, including Table S1†). The ligand adopts a U-shape conformation and intermolecular interactions mostly consist of hydrogen bonding contacts, the most notable being homoleptic amide···amide and triazole···triazole synthons. The amide nitrogen atom N5 donates a hydrogen bond to oxygen O3 of an adjacent molecule with an N5···O3 distance of 3.081 (2) Å and NH···O angle of 163.13(12)°. The triazole groups exhibit CH···N interactions from the acidic C–H site, with an N3···C9 distance of 3.412(3) Å and a C–H···N angle of 138.6 (2)°. Additional diffuse contacts involving the carbonyl oxygen atoms and various weaker C–H donor groups are also evident within the wider structure.

Following the successful synthesis of compounds **4** and **5**, the tris Tb(III) complexes $[Tb(\mathbf{4})_3]^{3+}$ and $[Tb(\mathbf{5})_3]^{3+}$ were prepared by reacting compounds **4** or **5** with Tb(III) under thermodynamic control. The complex $[Tb(\mathbf{4})_3]^{3+}$ was prepared by reacting 1 equivalent of $Tb(CF_3SO_3)_3$ with 3 equivalents of **4** in CH_3OH under microwave irradiation at 70 °C for 20 minutes. The resulting colourless solution was concentrated under reduced pressure and dropped slowly into a large excess of cold diethyl ether. The complex was then recovered by centrifugation from the diethyl ether supernatant solution and dried under high vacuum to generate the complex in 56% yield. Complex $[Tb(\mathbf{5})_3]^{3+}$ was prepared using the same procedure and also yielded a while solid in 43% yield.

Attempts were made to obtain crystals of the Tb(III) complexes under various conditions, unfortunately none were successful. The two complexes were also characterised by ^{1}H NMR in CD_3OD (see the ESI†). The paramagnetic nature of the Tb(III) ion resulted in significant broadening of the signals in $[Tb(\mathbf{4})_3]^{3+}$, with no significant chemical shifts seen in the ^{1}H NMR of the complex *vs.* that of the free ligand. This small chemical shift was also observed in previous work where we use **btp** ligands.

The successful formation of the $[Tb(\mathbf{4})_3](CF_3SO_3)_3$ complex was verified by elemental analysis (see the Experimental section). However, we were unable to detect evidence of the $[Tb(\mathbf{4})_3]^{3+}$ ion using MALDI HRMS (see the ESI†). This we often experience, as the complex can lose ligands during the HRMS experiment. Similarly, $[Tb(\mathbf{5})_3](CF_3SO_3)_3$ was not observed in MALDI HRMS, but $[Tb(\mathbf{5})_2(CF_3SO_3)_2]^+$ was observed (see the ESI†), and it is quite possible that the dissociation of the complex occurred. Elemental analysis confirmed the presence of the tris-complex in both cases ($[Tb(\mathbf{4})_3]^{3+}$ and $[Tb(\mathbf{5})_3]^{3+}$). The IR spectra of the solid complexes were recorded and a decrease in the stretching frequency of the carbonyl functional group was observed from 1637 to 1585 cm^{-1} and a C–F stretch

appeared at 1278 cm^{-1} in the case of $[Tb(\mathbf{4})_3]^{3+}$, further indicating the successful complexation of **4** with Tb(III). Similar changes were observed in the IR spectra of compound **5** and $[Tb(\mathbf{5})_3]^{3+}$.

Photophysical characterisation of complexes $[Tb(\mathbf{4})_3]^{3+}$ and $[Tb(\mathbf{5})_3]^{3+}$

After obtaining the two Tb(III) complexes ($[Tb(\mathbf{4})_3]^{3+}$ and $[Tb(\mathbf{5})_3]^{3+}$) their photophysical properties were investigated in CH_3CN solution. The UV-visible absorption and the excitation spectra of the two complexes were dominated by two main broad absorption bands that were centred at λ = 245 nm and λ = 293 nm (see the ESI†). These bands can be assigned to π–π^* transitions in the ligand structure. The fluorescence emission spectra were also recorded (see further discussion below), showing a ligand centred emission centred at around 350 nm. The excitation spectra (using Tb(III) λ_{em} at 545 nm) were structurally similar to the absorption spectra (see overlapped spectra in the ESI†), indicating that the excitation of the ligand gave rise to energy transfer to the Tb(III) excited state. Furthermore, this Tb(III)-centred emission was also clearly visible to the naked eye as seen in the inset in Fig. 4.

The sensitisation of the Tb(III) excited state was confirmed by observing the delayed emission at λ = 255 nm which showed the presence of Tb(III)-centred luminescence in both complexes indicating effective population of the $^5D_4$ excited state of the Ln(III) ion and subsequent deactivation of the ^7F_J (J = 6–2) ground states with line-like emission bands appearing at 490 nm, 545 nm, 584 nm, 622 nm and 645 nm, the latter of which was very weak, as can be seen in Fig. 4 for $[Tb(\mathbf{4})_3]^{3+}$ (see the ESI† for $[Tb(\mathbf{5})_3]^{3+}$).

To understand further the coordination environment around the lanthanide, the Tb(III) centred luminescence lifetimes (τ_{obs}) were recorded for $[Tb(\mathbf{4})_3]^{3+}$ and $[Tb(\mathbf{5})_3]^{3+}$ in H_2O and D_2O in which the complexes were sparingly soluble. The emission decay (at λ_{em} = 545 nm) was measured at various gate times upon excitation of the ligand, and the average radiative lifetimes of the delayed emission were calculated from the decay. The lifetimes of the $^5D_4$ excited state of Tb(III) were best fitted as a bi-exponential decay for $[Tb(\mathbf{4})_3]^{3+}$ and $[Tb(\mathbf{5})_3]^{3+}$ in H_2O and D_2O which indicates that there was more than one emissive species in solution. These results are summarised in Table 1.

Upon repetition of the experiment in CH_3OH and CD_3OD, in which the complexes were fully soluble, the lifetimes were the best fit to a mono-exponential decay for both complexes, indicating that there was a single emissive species in solution. This is likely due to the improved stability of $[Tb(\mathbf{4})_3]^{3+}$ and $[Tb(\mathbf{5})_3]^{3+}$ in methanolic solution which likely prevents any degree of dissociation of the tris complex, as occurring in aqueous solution.

From the fit decay curves, the excited state lifetimes in H_2O and D_2O as well as CH_3OH and CD_3OD were determined (Table S1†). From these data the hydration state (the number of metal ion bound water molecules), q, was also determined.[28,29] From this analysis, the q value determined for $[Tb(\mathbf{4})_3]^{3+}$ in an aqueous suspension was ~3. While this determination has large errors due to the poor solubility, the analysis would imply that three water molecules were bound to the Tb(III)-centre. This could also suggest the presence of the ML_2 species in the suspension as we had observed before in HRMS. Being highly competitive media, this could also indicate that the complex undergoes ligand dissociation in aqueous media. As mentioned, then the fitting of the excited state decay was best fit to bi-exponential decay, and from the fit, a second shorter lifetime was observed from which a q value of approximately 6 was determined, which could be speculated to be due to the presence of a ML species in solution. This would also contribute to the poor luminescence of this system in water where the $^5D_4$ excited state of Tb(III) is quenched by O–H oscillators.[30] However, in methanolic solution, in which the complex was stable, the decay was mono-exponential, and using Horrocks' equation, the hydration state was determined to be approximately zero. This suggests that in this less competitive solution, the full coordination requirement of the Tb(III) was fulfilled by the ligand and the ML_3 species was formed. The same trend and outcome were also observed upon determining the hydration states obtained for $[Tb(\mathbf{5})_3]^{3+}$ (see ESI Table S2†).

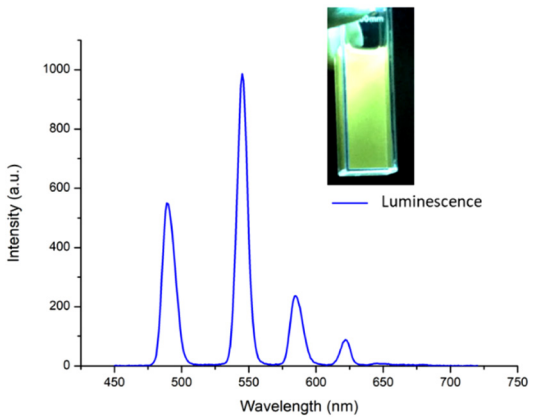

Fig. 4 The delayed luminescence spectra of $[Tb(\mathbf{4})_3]^{3+}$(2.7×10^{-5} M) recorded in CH_3CN showing the characteristic Tb(III) transitions $^5D_4 \rightarrow {}^7F_{6,5,4,3,2}$. Inset: green Tb(III) emission that was visible to the naked eye upon placing the sample under a UV-Vis lamp.

Table 1 Luminescence lifetimes (τ) recorded from aqueous suspensions and methanolic solutions of $[Tb(\mathbf{4})_3]^{3+}$ and $[Tb(\mathbf{5})_3]^{3+}$ with q-values (hydration states). The data for $[Tb(\mathbf{6})_3]^{3+}$ are also shown

Complex	τ (H_2O), ms	τ (D_2O), ms	τ (CH_3OH), ms	τ (CD_3OD), ms	q (±0.5)
$[Tb(\mathbf{4})_3]^{3+}$			1.905	2.213	0.13
$[Tb(\mathbf{5})_3]^{3+}$			1.943	2.463	0.52
$[Tb(\mathbf{4})_3]^{3+}$ τ_1	0.401	0.751			5.53
$[Tb(\mathbf{4})_3]^{3+}$ τ_2	1.095	2.865			2.52
$[Tb(\mathbf{5})_3]^{3+}$ τ_1	0.376	0.749			6.32
$[Tb(\mathbf{5})_3]^{3+}$ τ_2	1.014	2.424			2.56
$[Tb(\mathbf{6})_3]^{3+}$	1.561	2.203			0.63

The quantum yield (Φ_{tot})‡ was also determined for both complexes (λ_{ex} at 255 nm), and found to be 84.0(7)% for $[Tb(\mathbf{4})_3]^{3+}$. This is similar to that observed for most Tb(III) based **btp** complexes that have high Φ_{tot}. However, in contrast, the $[Tb(\mathbf{5})_3]^{3+}$ complex was found to be significantly less emissive with Φ_{tot} = 15.3(7)%. This is, however, in line with our previous observation that a **btp** based-Trp ligand appears to be a poor sensitizer for Tb(III) when compared to its Phe counterpart.[26]

The above results demonstrate that Tb(III) is in general a 'good lanthanide ion' for use in the formation of **tzpa** based complexes and that the photophysical properties of these systems mirror those generated by **btp** ligands. Unfortunately, the stability of these complexes in aqueous solution was not desirable, while they showed good stability in both CH_3CN and MeOH solutions where the coordination environment is fully saturated.

Observing the self-assembly formation between 4 and 5 and Tb(III) under kinetic control

Having probed the photophysical properties of the two complexes $[Tb(\mathbf{4})_3]^{3+}$ and $[Tb(\mathbf{5})_3]^{3+}$ that formed under microwave-aided synthesis, the Tb(III) directed self-assembly of **4** and **5** with $Tb(CF_3SO_3)_3$ was investigated *in situ* by carrying out a series of spectroscopic measurements (*i.e.* under kinetic control) under ambient conditions. Our previous work in this area has shown that these assemblies tend to be more dynamic and varied in stoichiometry. The main focus here will be on discussing the changes observed using **4**. (The changes seen for **5** are given in the ESI.†) To probe these changes, specific aliquots of Tb(III) equivalents (in solution) were added to a solution of **4** (1×10^{-5} M) and the changes in the UV-visible absorption, fluorescence and delayed Tb(III) luminescence spectra were monitored in CH_3CN solution. All measurements were repeated three times to ensure full reproducibility.

Ground state and fluorescence emission changes. The UV-visible absorption of compound **4** showed two main bands in the absorbance spectrum. A high-energy band was centred at λ = 245 nm while a lower energy band was observed at λ = 291 nm (ε = 24 100 cm^{-1} M^{-1} at λ_{abs} = 242 nm). Upon addition of Tb(III), the band centred at λ = 245 nm experienced a hypochromic shift and the appearance of a new band at λ = 225 nm was also observed, as demonstrated in Fig. 5. These changes reached a maximum at approximately 0.5 equivalents of Tb(III), after which no further significant changes occurred. The low energy band at λ = 291 nm showed a hyperchromic shift and a concomitant redshift to λ = 300 nm upon the addition of Tb (III). Again, these changes reached a plateau at the addition of 0.5 equivalents of Tb(III). Two isosbestic points were observed at λ = 236 nm and λ = 290 nm, indicating the presence of multiple correlated species in solution. Similarly, for **5**, the main changes occurred up to the addition of 0.5 equivalents of Tb(III) after which they reached a plateau (see the ESI†).

Upon excitation of ligand **4** at λ = 255 nm, the ligand gave rise to broad fluorescence emission with λ = 353 nm, Fig. 5. Upon the addition of Tb(III), the ligand fluorescence was significantly affected by the complexation process, becoming gradually quenched, with *ca.* 70% reduction in the fluorescence emission intensity at the addition of 0.5 equivalents of Tb(III), Fig. 5. In fact, by the addition of 0.7 equivalents of Tb(III) the fluorescence was fully quenched. As before, this can be attributed to an energy transfer process from ligand **4** to the Tb(III) metal centre which gives rise to Tb(III)-centred emission. Indeed this we observed as discussed next. Again, similar results were observed in the fluorescence emission spectra of **5** upon titrating with Tb(III) (see the ESI†). However, the emission was fully quenched by the addition of 0.5 equivalents of Tb(III).

Lanthanide luminescence changes. The changes in the delayed Tb(III)-centred emission were recorded upon the excitation of **4** at λ = 255 nm. The spectra and binding isotherms can be seen in Fig. 6 demonstrating a gradual enhancement in the Tb(III)-centred transitions at λ = 490, 545, 584, 622, 648, 667 and 679 nm, upon deactivation of the $^5D_4$ state to the ^7F_J (J = 6–0) states, respectively. As shown in Fig. 6, emission gradually enhanced up to the addition of 0.5 equivalents of Tb(III). Subsequent additions resulted, however, in some degree of quenching of the Tb(III) emission. The changes in the Tb(III) emission upon titrating **5** were also monitored concomitantly (see the ESI†). However, unlike that seen for **4**, no significant enhancement was observed in the Tb(III)-centred emission before the addition of 0.5 equivalents of Tb(III), after which, the emission increased dramatically and continued to increase beyond 5 equivalents of Tb(III). This could be due to slow kinetics under ambient conditions.

Fitting the spectroscopic changes using non-linear regression analysis. With the view of shedding light on the changes above, and to explore which stoichiometries dominated in solution, the above data were analysed by using non-linear regression analysis, and the speciation in solution as well as the stability constants estimated from the global analysis (using ReactLab EQUILIBRIA software). Initially, we fitted the changes to the UV-visible absorption spectrum. Analysis of the UV-visible absorption titration data for ligand **4** with $Tb(CF_3SO_3)_3$ pointed to the presence of four main species (**4**, 1 : 1 metal : ligand species, 1 : 2 metal : ligand species and 1 : 3 M : L species) in solution as shown in Fig. 7. The distribution of these species was estimated in the analysis, which showed that from 0 → 0.25 equivalents of Tb(III), both the 1 : 2 metal : ligand and 1 : 3 metal : ligand species co-exist in solution, both reaching approximately 25% abundance. However, the subsequent additions of Tb(III) resulted in a decrease in the abundance of the ML_3 species while the ML_2 species continued to increase, reaching 92% abundance at 0.5 equivalents of Tb(III). From 0.5 → 3 equivalents, the ML_2 underwent gradual dis-

‡The photoluminescence quantum yield (Φ_{tot}, %) was determined in CH_3CN using a relative method against a standard developed by Bünzli and co-workers.[30] This relative method for quantum yield determination is described in the following equation:

$$\phi_{REL}^{Tb,L} = \frac{\phi_S}{\phi_R} \times \frac{E_S}{E_R} \times \frac{A_R(\lambda R)}{A_S(\lambda S)} \times \frac{I_R(\lambda R)}{I_S(\lambda S)} \times \frac{{n_S}^2}{{n_R}^2}$$

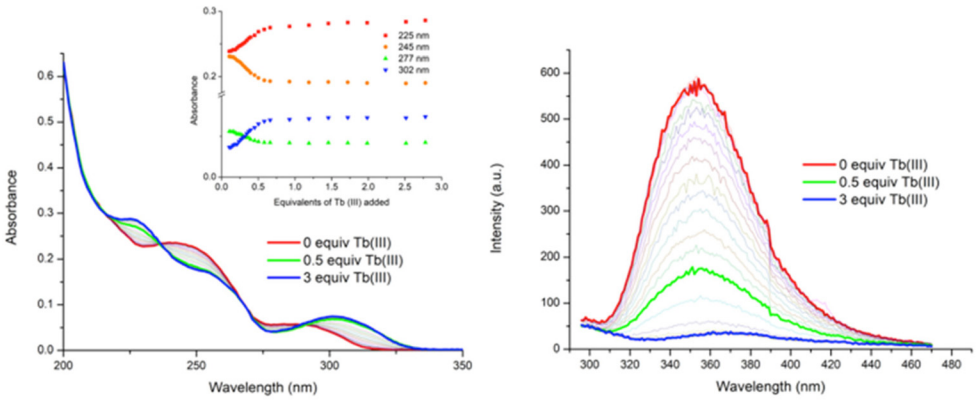

Fig. 5 The observed spectroscopic changes for **4** (1×10^{-5} M) against $Tb(CF_3SO_3)_3$ (0 → 3 equiv.) in CH_3CN at RT. (Left) the UV-visible absorption spectra. Inset: corresponding experimental binding isotherms with absorbance at λ = 225, 245, 277 and 300 nm. (Right) the corresponding changes in the fluorescence emission spectra, λ_{ex} = 255 nm.

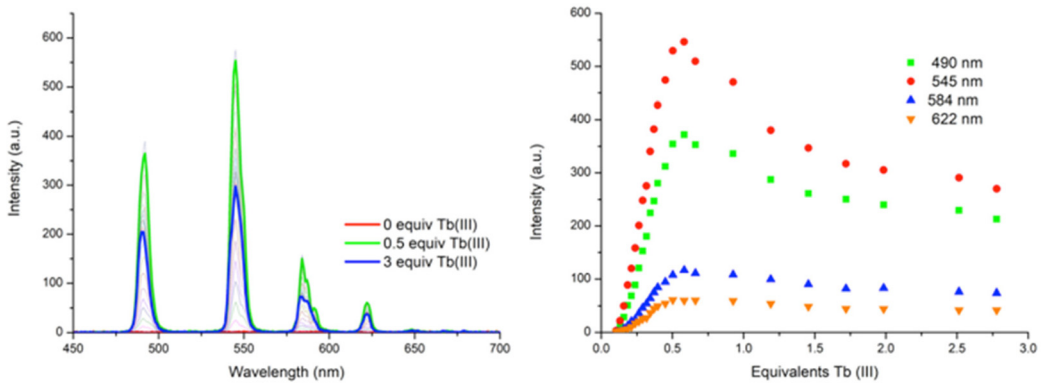

Fig. 6 (Left) The overall changes to the Tb(III)-centred emission spectra upon titrating **4** (1×10^{-5} M) against $Tb(CF_3SO_3)_3$ (0 → 3 equiv.) in CH_3CN at RT. (Right) The corresponding experimental binding isotherms for the Tb(III) emission at λ = 492, 545, 585 and 623 nm.

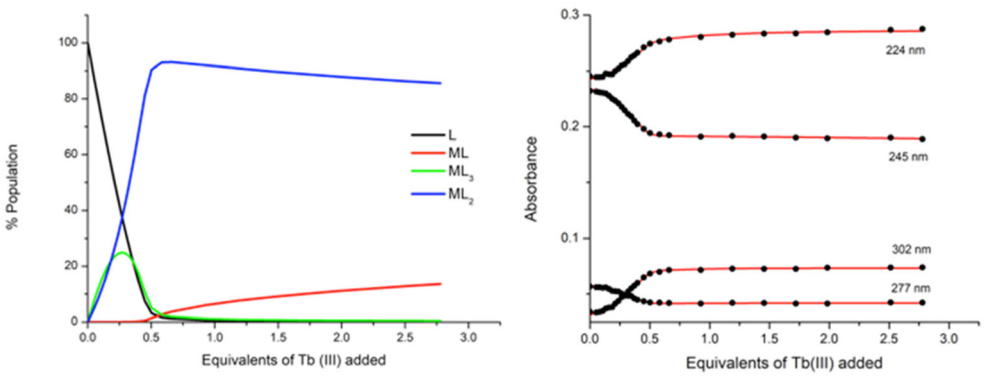

Fig. 7 (Left) the speciation distribution diagram obtained from the fit of the UV-visible absorption titration data of ligand **4** against $Tb(CF_3SO_3)_3$ in CH_3CN. (Right) the fit of the experimental binding isotherms using non-linear regression analysis software ReactLab.

sociation into the ML species due to the presence of excess metal ions in solution. And while the ML_3 species is likely the most emissive species in solution due to the exclusion of solvent molecules from the inner coordination sphere of the Tb(III) ion, the ML_2 species is formed more favourably at this low concentration under kinetic control.

The stepwise binding constants were estimated for each species from the changes in the UV-visible absorption spectra

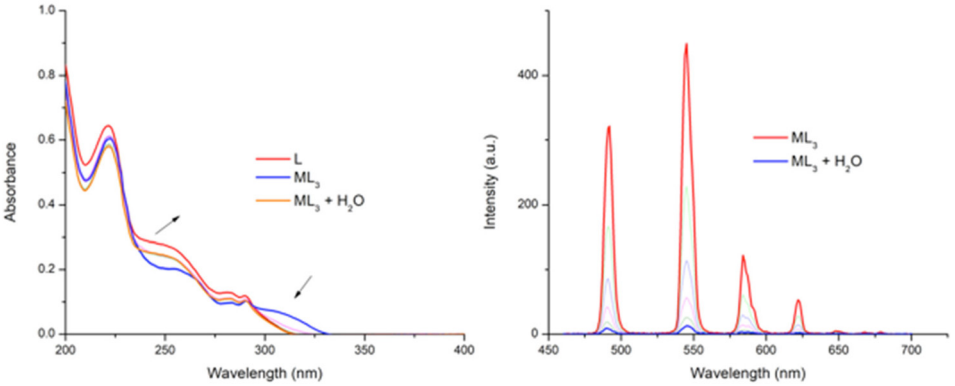

Fig. 8 (Left) Absorbance spectra of ligand **6** upon addition of Tb(III) at 0 and 3 equivalents of Tb(III), and upon addition of H_2O. (Right) the Tb(III) emission spectrum of the 1 : 3 complex showing decrease in luminescence intensity upon the addition of H_2O.

throughout the titration and are expressed here as $\log \beta_{ML}$. The 1 : 2 metal : ligand species formed with $\log \beta_{12}$ = 14.4 and the 1 : 3 metal : ligand species had a calculated binding constant of $\log \beta_{13}$ = 19.5 while the ML species was estimated as $\log \beta_{11}$ = 6.3 ± 0.1.

In a similar manner, the analysis of **5** with Tb(III) pointed to the presence of four main species in solution upon fitting the changes in the ground state (see the ESI†). The distribution of these species was also estimated from the analysis and indicates that from 0 → 0.5 equivalents of Tb(III), both the ML_2 and ML_3 species coexist in solution. However, the ML_3 species reaches a maximum abundance of 12% at 0.25 equivalents of Tb(III), while the ML_2 species is significantly more dominant at 94% abundance upon the addition of 0.5 equivalents of Tb(III). Subsequent additions of Tb(III) resulted in a gradual dissociation of the ML_2 species into the less emissive ML species. Binding constants were estimated from the analysis and the ML_3 species was found to form with $\log \beta_{13}$ = 19.2 ± 0.2 while the ML_2 species had a calculated binding constant of $\log \beta_{12}$ = 14.6 ± 0.2 and finally, the ML species was calculated as $\log \beta_{11}$ = 6.6 ± 0.1. These values are in good agreement with those seen for **4** above indicating that the amino acid moiety does not have a large influence on the self-assembly in solution.

Unfortunately, while attempts were made to obtain fits for either the fluorescence or the Tb(III) luminescence titration data obtained for **4** and **5**, they did not result in data convergence and reliable binding constants could not be obtained.

Probing the interaction of Tb(III) with ligand 6

Having examined the amino ester derivatives **4** and **5**, we also investigated the ability of the hydrolysed ligand **6** to interact with Tb(III), and to see if the carboxylic acid had any effect on the self-assembly formation with Tb(III) under kinetic control, the measurements were carried out in CH_3CN. The changes in the absorption and the Tb(III) emission are shown in Fig. 8 upon the addition of 3 equivalents of lanthanide. Initially, the 1 : 3 complex was found to be stable in CH_3CN solution over 24 hours (by monitoring the UV-visible absorption spectra), with no changes being observed over the duration. Furthermore, lifetime and *q*-value determination (Table 1) showed that the excited state decay was best fitted to a mono-exponential decay, and that the *q* value was ~0. Given the improved solubility of the ligand **6** in competitive media we titrated water into this solution. However, this, as the changes in Fig. 8 demonstrate, resulted in the dissociation of the self-assembly, where the UV-visible absorption spectrum returns to the absorbance profile of ligand **6**. Similarly, the Tb(III) emission intensity was also gradually quenched upon the addition of H_2O.

Conclusion

The synthesis of two new **tzpa** ligands **4** and **5** from the α-amino acid (*S*) L-phenylalanine or L-tryptophan (as their methyl esters) was achieved in a few step synthesis. The solid-state crystal structure of **4** was also obtained. The hydrolysis of the amino ester **4** also produced ligand **6**. Both ligands **4** and **5** were shown to form 1 : 3 complexes with Tb(III) under thermodynamic control, which were highly luminescent, and the green Tb(III) emission was clearly visible to the naked eye. In contrast to this, under kinetic control, the global analysis of the titration data obtained from the ground state changes with Tb(III) showed that for both **4** and **5**, the 1 : 2 stoichiometry dominated for both systems after the addition of 0.5 equivalents of the ion. This was also confirmed by investigating the excited state lifetimes of the Tb(III) centred emission. From these changes we were able to determine both the binding affinity and the stoichiometry in solution. This 'in solution' (titration) behaviour is different to that obtained normally for either **btp** or **dpa** ligands based on which the **tzpa** structure is modelled, where the 1 : 3 stoichiometry is dominant under both thermodynamic and kinetic conditions. Both ligands provide a platform to explore the chemistry of the **tzpa** structure further in supramolecular and coordination chemistries, an endeavour which we are currently engaged in. By structurally modulating both the carboxylic site as well as the triazole moiety (*e.g.* both *X* and *Y* sites, Fig. 1), the formation of

dimeric ligand structures that can be used in the formation of dimetallic helicates and other supramolecular structures is currently being undertaken in our laboratory.

Experimental

Methyl-6-bromopicolinate (1)

6-Bromopicolinic acid (3.0 g, 14.85 mmol) was suspended in MeOH (5 mL) and 4 drops of sulfuric acid were added. The mixture was heated to reflux for four hours and quenched with $NaHCO_3$ in water. The product was extracted into DCM, washed with sodium hydrogen carbonate solution and dried over magnesium sulphate to yield a white solid (2.095 g, 9.65 mmol, 77%). The product decomposed over 91 °C. HRMS (*m*/*z*) (ESI+): calculated for $C_7H_7BrNO_2^+$ *m*/*z* = 215.9660 $[M + H]^+$. Found *m*/*z* = 215.9654; ^{1}H NMR (400 MHz, $CDCl_3$-d_6): δ (ppm) = 8.10 (dd, *J* = 6.7, 1.8 Hz, 1H, 3-pyr H), 7.69 (t, *J* = 6.7, 2H, 4-pyr H),7.70 (dd, *J* = 6.7, 1.8 Hz, 1H, 5-pyr H), 4.00 (s, 3H, OCH_3). ^{13}C NMR (150 MHz, DMSO-d_6): δ (ppm) = 163.8, 148.1, 141.3, 140.9, 132.1, 124.5, 52.8; IR ν_{max} (cm^{-1}): 3106, 2968, 1718, 1556, 1437, 1422, 1310, 1246, 1132, 1113, 985, 955, 757, 732.

Methyl 6-((trimethylsilyl)ethynyl)picolinate (2)

To a solution of **1** (1.650 g, 7.60 mmol) in THF/NEt_3 4 : 1, 40 (mL), in the presence of CuI (0.2 mmol) and $Pd(PPh_3)_4$ (0.2 mmol), ethynyltrimethylsilane (1.1 mL, 7.60 mmol) was added dropwise at 0 °C under an argon atmosphere. The resulting solution was left to stir at room temperature for 48 h, after which the solution was filtered through a plug of Celite and concentrated under reduced pressure to yield a brown solid which was purified by flash column chromatography (RediSep® 12 g, gradient elution 0 → 90% EtOAc in hexane). This gave **2** as a brown solid in 65% yield (1.158 g, 4.94 mmol). The product decomposes over 85 °C. HRMS (*m*/*z*) (ESI+): calculated for $C_{12}H_{15}NO_2Si^+$ *m*/*z* = 234.0950 $[M + H]^+$. Found *m*/*z* = 234.0963; ^{1}H NMR (400 MHz, $CDCl_3$-d_6): δ (ppm) = 8.06 (d, *J* = 7.6 Hz, 1H, 3-pyr H), 7.80 (t, *J* = 8.1, 7.6 Hz, 1H, 4-pyr H), 7.63 (d, *J* = 8.1 Hz, 1H, 5-pyr H), 4.00 (s, 3H, OCH_3), 0.26 (s, 9H, Si-$(CH_3)_3$). ^{13}C NMR (150 MHz, DMSO-d_6): δ (ppm) = 164.6, 147.8, 141.8, 138.5, 130.5, 124.6, 103.3, 95.1, 52.6, 0.4.; IR ν_{max} (cm^{-1}): 3106, 3082, 2092, 1864, 1736, 1577, 1437, 1251, 840, 764.

4-((4-(6-(Methoxycarbonyl)pyridin-2-yl)-1*H*-1,2,3-triazol-1-yl) methyl)benzoic acid (3)

To a solution of 4-bromomethyl benzoic acid (1.418 g, 6.60 mmol) in 10 mL 4 : 1 DMF/water was added sodium azide (0.428 g, 6.60 mmol) and the reaction mixture was stirred for one hour to yield the azide intermediate that was not isolated and therefore used without further purification. To this solution was added ligand **2** (1.539 g, 6.560 mmol), $CuSO_4{\cdot}5H_2O$ (0.329 g, 1.32 mmol), sodium ascorbate (0.522 g, 2.64 mmol) and anhydrous K_2CO_3 (0.912 g, 6.60 mmol) and stirred at room temperature under an argon atmosphere overnight. 1 M EDTA/NH_4OH solution was added to the mixture and the product was precipitated using 1M HCl and filtered to yield an off-white solid. The product was used without further purification. (1.562 g, 4.62 mmol, 70%). HRMS (*m*/*z*) (ESI+): calculated for $C_{17}H_{14}N_4O_4H^+$ *m*/*z* = 339.1093 $[M + H]^+$. Found *m*/*z* = 339.1087; ^{1}H NMR (400 MHz, DMSO-d_6): δ (ppm) = 8.82 (s, 1H, triazole CH), 8.26 (dd, *J* = 7.8, 1.1 Hz, 1H, 5-pyr H), 8.10 (s, *J* = 7.8, 1H, 4-pyr *H*), 8.00 (dd, *J* = 7.8, 1.1 Hz, 1H, 3-pyr H), 7.95 (d, *J* = 8.4 Hz, 2H, Ar*H*-COOH), 7.47 (d, *J* = 8.4 Hz, 2H, Ar*H*-CH_2), 5.79 (s, 2H, CH_2-Ar), 3.90 (s, 3H, COO-CH_3). ^{13}C NMR (150 MHz, DMSO-d_6): δ (ppm) = 170.1, 165.6, 150.2, 147.6, 146.8, 137.2, 138.7, 135.3, 129.2, 128.1, 124.1, 123.9, 123.1, 52.7.; IR ν_{max} (cm^{-1}): 1725, 1612, 3215, 1282, 1126, 1011, 776, 707.

General experimental procedure for amino acid coupling to 3

To a solution of the relevant amine (1 equivalent) in a DMF : DCM (4 : 1) mixture under argon were added HOBt (1 equivalent), NEt_3 (1.2 equivalents) and the relevant acid (1.1 equivalents). The reaction mixture was stirred for 30 min and cooled to 0 °C. EDC·HCl (1.5 equivalents) was then added to the suspension and stirred at 0 °C for a further 30 min. The mixture was then allowed to warm to room temperature and stirred for a further 48 h.

Methyl(*S*)-6-(1-(4-((1-methoxy-1-oxo-3-phenylpropan-2-yl) carbamoyl)benzyl)-1*H*-1,2,3-triazol-4-yl)picolinate (4)

Synthesised according to the general procedure mentioned above from phenylalanine hydrochloride (0.99 g, 4.91 mmol) and compound **3** (1.512 g, 4.47 mmol) to yield a white solid (1.611 g, 3.26 mmol, 72%). The product decomposes over 207 °C. HRMS (*m*/*z*) (ESI+): calculated for $C_{27}H_{25}N_5O_5Na^+$ *m*/*z* = 522.1753 $[M + Na]^+$. Found *m*/*z* = 522.1767; ^{1}H NMR (600 MHz, DMSO-d_6): δ (ppm) = 8.86 (d, *J* = 8.1 Hz, 1H, NH), 8.80 (s, 1H, triazole H), 8.26 (d, *J* = 1.1, 7.7 Hz, 1H, 5-pyr H), 8.10 (m, *J* = 1.1 Hz, 1H, 4-pyr *H*), 8.01 (d, *J* = 1.1, 7.7 Hz, 1H, 3-pyr H), 7.80 (d, *J* = 8.3 Hz, 2H, Ar *H*–C═O), 7.46 (d, *J* = 8.3 Hz, 2H, Ar *H*-CH_2), 7.28 (m, 4H, phe H), 7.19 (s, 1H, phe H), 5.76 (s, 2H, CH_2), 4.65 (s, *J* = 8.1 Hz, 1H, C*H*-NH), 3.91 (s, 3H, pyr-COOCH_3), 3.63 (s, 3H, $COOCH_3$), 3.23–2.97 (m, 2H, CH_2-Phe). ^{13}C NMR (150 MHz, DMSO-d_6): δ (ppm) = 172.1, 165.9, 165.0, 150.1, 147.6, 146.7, 139.2, 138.7, 137.6, 133.5, 129.0, 128.2, 127.9, 127.9, 126.5, 124.1, 123.8, 122.9, 54.2, 52.6, 52.5, 51.9, 36.2; IR ν_{max} (cm^{-1}): 3314, 1732, 1719, 1637, 1600, 1539, 1438, 1349, 1246, 1135, 1221, 1006, 825, 776, 752, 706, 644.

(*S*)-6-(1-(4-((1-Carboxy-2-phenylethyl)carbamoyl)benzyl)-1*H*-1,2,3-triazol-4-yl)picolinic acid (6)

Compound **4** (1.611 g, 3.23 mmol) was suspended in 1M NaOH and refluxed for 3 hours. The product was isolated by neutralization of the solution with acetic acid and filtration to yield a white solid (1.278 g, 2.72 mmol, 84%). HRMS (*m*/*z*) (ESI+): calculated for $C_{25}H_{21}N_5O_5Na^+$ *m*/*z* = 494.1440 $[M + Na]^+$. Found *m*/*z* = 494.1459; ^{1}H NMR (400 MHz, DMSO-d_6): δ (ppm) = 8.77 (s, 1H, triazole H), 8.25 (s, 1H, NH), 8.00 (d, *J* = 8.1 Hz, 1H, 5-pyr H), 7.91 (m, *J* = 7.6, 8.1 Hz, 1H, 4-pyr H), 7.85 (d, *J* =

7.6 Hz, 1H, 3-pyr H), 7.73 (d, J = 8.2 Hz, 2H, Ar H–C═O), 7.42 (d, J = 8.2 Hz, 2H, Ar H-CH_2), 7.23–7.07 (m, 5H, phe H), 5.74 (s, 2H, CH_2), 4.33 (s, 1H, CH-NH), 3.04 (dd, 2H, CH_2-Ph); ^{13}C NMR (150 MHz, DMSO-d_6): δ (ppm) = 173.10, 167.22, 165.79, 154.12, 149.30, 149.27, 147.75, 139.22, 139.13, 138.37, 134.84, 129.69, 128.40, 128.08, 126.48, 124.37, 123.41, 121.20, 55.29, 53.16, 37.24.; IR ν_{max} (cm^{-1}): 3355, 3059, 2436, 1960, 1736, 1634, 1535, 1503, 1381, 1180, 1052, 851, 812, 737.

Methyl (*S*)-6-(1-(4-((3-(1*H*-indol-3-yl)-1-methoxy-1-oxopropan-2-yl)carbamoyl)benzyl)-1*H*-1,2,3-triazol-4-yl)picolinate (5)

Synthesised according to the general procedure mentioned above using tryptophan hydrochloride (0.15 g, 0.59 mmol) and compound **3** (0.20 g, 0.59 mmol) to yield compound **5** as a white solid (0.20 g, 63%); HRMS (m/z) (ESI+): $C_{29}H_{26}N_6O_5^+$ m/z = 538.1965 [M + H]$^+$. Found m/z = 539.2037; ^{1}H NMR (600 MHz, DMSO-d_6): δ (ppm) = 10.80 (s, 1H, NH), 8.81 (s, 1H, NH), 8.79 (s, 1H, triazole H), 8.26 (d, J = 7.9 Hz, 1H, Ha), 8.10 (t, J = 7.8 Hz, 1H, Hb), 8.00 (d, J = 7.7 Hz, 1H, Hc), 7.82 (d, J = 8.2 Hz, 2H, Phe-CH_2), 7.54 (d, J = 7.9 Hz, 1H, Hd), 7.46 (d, J = 8.2 Hz, 2H, Phe-C═O), 7.31 (d, J = 8.1 Hz, 1H, Hg), 7.18 (s, 1H, Hh), 7.05 (t, J = 7.5 Hz, 1H, Hg), 6.97 (t, J = 7.4 Hz, 1H, He), 5.75 (s, 2H, CH_2-triazole), 4.67 (d, J = 5.4 Hz, 1H, CH), 3.91 (s, 3H, CH_3-pyr), 3.62 (s, 3H, CH_3-Tryp), 3.24 (ddd, J = 23.9, 14.6, 7.3 Hz, 2H, CH_2-Tryp); ^{13}C NMR (150 MHz, DMSO-d_6): δ (ppm) = 172.9, 166.5, 165.5, 150.6, 148.1, 147.1, 139.6, 139.2, 136.6, 134.1, 128.4, 124.6, 124.4, 124.1, 123.4, 121.4, 118.9, 118.5, 111.9, 110.4, 54.3, 53.1, 52.9, 52.4, 27.1; IR ν_{max} (cm^{-1}): 3403, 3297, 3150, 3049, 2948, 2923, 2841, 1739, 1627, 1602, 1531, 1450, 1369, 1253, 1217, 1147, 1055, 1010, 974, 772, 737, 696, 600.

Synthesis of Tb·4_3

Ligand **4** (10 mg, 0.02 mmol) was added to $Tb(CF_3SO_3)_3$ (5 mg, 0.007 mmol) in CH_3OH (5 mL) and heated at 70 °C under microwave irradiation for 15 minutes. The resulting solution was dried under vacuum to yield a colourless oil which was taken up in CH_3OH and dropped slowly into a large excess of swirling Et_2O to afford Tb·4_3 as a white solid in 56% yield. The ^{1}H NMR spectra were broad and are shown in the ESI. HRMS (m/z) (ESI+): $C_{56}H_{50}N_{10}O_{16}F_6S_2Tb$ m/z = 1455.2005 [Tb(**4**)$_2$(CF$_3$SO$_3$)$_2$]$^+$. Found m/z = 1455.2075; elemental analysis for $C_{84}H_{75}N_{15}O_{24}F_9S_3Tb{\cdot}4H_2O{\cdot}CH_3OH$ calculated: C 46.22 H 3.97 N 9.51; found: C 45.70 H 3.45 N 9.55.

Synthesis of Tb·5_3

Ligand **5** (10 mg, 0.02 mmol) was added to $Tb(CF_3SO_3)_3$ (5 mg, 0.007 mmol) in CH_3OH (5 mL) and heated at 70 C under microwave irradiation for 15 minutes. The resultant solution was dried under vacuum to yield colorless oil which was taken up in CH_3OH and dropped slowly into a large excess of swirling Et_2O to afford Tb·5_3 as a white solid in 43% yield. The ^{1}H NMR spectrum was broad and is shown in the ESI.† HRMS (m/z) (ESI+): $C_{60}H_{52}N_{12}O_{16}F_6S_2Tb$ m/z = 1533.2223 [Tb(**7**)$_2$(CF$_3$SO$_3$)$_2$]$^-$ found m/z = 1533.2262.

Conflicts of interest

There are no conflicts to declare.

Acknowledgements

The authors gratefully acknowledge the Science Foundation Ireland (SFI PI Award 13/1A/1865 to TG) and the School of Chemistry, Trinity College Dublin for financial support. We thank Dr Gary Hessman for MS characterisation, Dr John O'Brien for NMR spectroscopy and Dr Manuel Ruether for instrumental support.

References

1 (*a*) J. Dong, Y. Liu and Y. Cui, Supramolecular chirality in metal-organic complexes, *Acc. Chem. Res.*, 2021, **54**, 194; (*b*) C.-T. Yeung, K.-H. Yim, H.-Y. Wong, R. Pal, W.-S. Lo, S.-C. Yan, M. Yee-Man Wong, D. Yufit, D. E. Smiles, L. J. McCormick, S. J. Teat, D. K. Shuh, W.-T. Wong and G.-L. Law, Chiral transcription in self-assembled tetrahedral Eu4L6 chiral cages displaying sizable circularly polarized luminescence, *Nat. Commun.*, 2017, **8**, 1128; (*c*) D. A. Roberts, B. S. Pilgrim and J. R. Nitschke, Covalent post-assembly modification in metallosupramolecular chemistry, *Chem. Soc. Rev.*, 2018, **47**, 626; (*d*) A. J. Savyasachi, O. Kotova, S. Shanmugaraju, S. J. Bradberry, G. M. Ó'Máille and T. Gunnlaugsson, Supramolecular Chemistry: A Toolkit for Soft Functional Materials and Organic Particles, *Chem*, 2017, **3**, 764.

2 (*a*) X.-Y. Luo and M. Pan, Metal-organic materials with circularly polarized luminescence, *Coord. Chem. Rev.*, 2022, **468**, 214640; (*b*) J. Gong and X. Zhang, Coordination-based circularly polarized luminescence emitters: Design strategy and application in sensing, *Coord. Chem. Rev.*, 2022, **453**, 214329; (*c*) D. E. Barry, D. F. Caffrey and T. Gunnlaugsson, Lanthanide-directed synthesis of luminescent self-assembly supramolecular structures and mechanically bonded systems from acyclic coordinating organic ligands, *Chem. Soc. Rev.*, 2016, **45**, 3244.

3 (*a*) L.-J. Chen, H.-B. Yang and M. Shionoya, Chiral metallosupramolecular architectures, *Chem. Soc. Rev.*, 2017, **46**, 2555; (*b*) A. M. Castilla, W. J. Ramsay and J. R. Nitschke, Stereochemistry in subcomponent self-assembly, *Acc. Chem. Res.*, 2014, **47**, 2063; (*c*) T. Sawada, A. Matsumoto and M. Fujita, Coordination-driven folding and assembly of a short peptide into a protein-like two-nanometer-sized channel, *Angew. Chem., Int. Ed.*, 2014, **53**, 7228; (*d*) C. M. G. dos Santos, A. J. Harte, S. J. Quinn and T. Gunnlaugsson, Recent developments in the field of supramolecular lanthanide luminescent sensors and self-assemblies, *Coord. Chem. Rev.*, 2008, **252**, 2512.

4 (*a*) Y. B. Tan, M. Yamada, S. Katao, Y. Nishikawa, F. Asanoma, J. Yuasa and T. Kawai, Self-assembled tetra-

nuclear EuIII complexes with D2- and C2h-symmetrical square scaffold, *Inorg. Chem.*, 2020, **59**, 12867; (*b*) J. Anhäuser, R. Puttreddy, Y. Lorenz, A. Schneider, M. Engeser, K. Rissanen and A. Lützen, Chiral self-sorting behaviour of [2.2]paracyclophane-based bis(pyridine) ligands, *Org. Chem. Front.*, 2019, **6**, 1226; (*c*) T. Gorai, W. Schmitt and T. Gunnlaugsson, Highlights of the development and application of luminescent lanthanide based coordination polymers, MOFs and functional nanomaterials, *Dalton Trans.*, 2021, **50**, 770; (*d*) J. A. Kitchen, Lanthanide-based self-assemblies of 2,6-pyridyldicarboxamide ligands: Recent advances and applications as next-generation luminescent and magnetic materials, *Coord. Chem. Rev.*, 2017, **340**, 232.

5 (*a*) Y. Wang, Y. Zhou, Z. Yao, W. Huang, T. Gao, P. Yan and H. Li, Asymmetric induction in quadruple-stranded europium(III) helicates and circularly polarized luminescence, *Dalton Trans.*, 2022, **51**, 10973; (*b*) S. D. Bonsall, M. Houcheime, D. A. Straus and G. Muller, Optical isomers of N, N′-bis(1-phenylethyl)-2,6-pyridinedicarboxamide coordinated to europium(III) ions as reliable circularly polarized luminescence calibration standards, *Chem. Commun.*, 2007, **35**, 3676.

6 (*a*) J. Jiao, J. Dong, Y. Li and Y. Cui, Fine-tuning of chiral microenvironments within triple-stranded helicates for enhanced enantioselectivity, *Angew. Chem., Int. Ed.*, 2021, **60**, 16568; (*b*) J.-K. Ou-Yang, Y.-Y. Zhang, M.-L. He, J.-T. Li, X. Li, X.-L. Zhao, C.-H. Wang, Y. Yu, D.-X. Wang, L. Xu and H.-B. Yang, Unexpected self-assembly of chiral triangles from 90° chiral di-Pt(II) acceptors, *Org. Lett.*, 2014, **16**, 664.

7 (*a*) R. Chen, Q.-Q. Yan, S.-J. Hu, X.-Q. Guo, L.-P. Zhou and Q.-F. Sun, Dinuclear mono-bridged or polymeric lanthanide complexes from one ligand: structural transformation and chiral induction, *Dalton Trans.*, 2023, **52**, 37; (*b*) L.-L. Yan, C.-H. Tan, G.-L. Zhang, L.-P. Zhou, J.-C. Bünzli and Q.-F. Sun, Stereocontrolled Self-Assembly and Self-Sorting of Luminescent Europium Tetrahedral Cages, *J. Am. Chem. Soc.*, 2015, **137**, 8550.

8 (*a*) D. Luo, X.-Z. Wang, C. Yang, X.-P. Zhou and D. Li, Self-assembly of chiral metal-organic tetartoid, *J. Am. Chem. Soc.*, 2018, **140**, 118; (*b*) E. Badetti, K. Wurst, G. Licini and C. Zonta, Multimetallic architectures from the self-assembly of amino acids and tris(2-pyridylmethyl)amine Zinc(II) Complexes: circular dichroism enhancement by Chromophores organization, *Chem. – Eur. J.*, 2016, **22**, 6515; (*c*) Y. Ye, T. R. Cook, S.-P. Wang, J. Wu, S. Li and P. J. Stang, Self-Assembly of chiral metallacycles and metallacages from a directionally adaptable BINOL-derived donor, *J. Am. Chem. Soc.*, 2015, **137**, 11896.

9 (*a*) T. Granch, C. Tourbillon, J. Ferrando-Soria, M. Julve, F. Lloret, J. Pasán, C. Ruiz-Pérez, O. Fabelo and E. Pardo, Self-assembly of a chiral three-dimensional manganese (II)-copper(II) coordination polymer with a double helical architecture, *CrystEngComm*, 2013, **15**, 9312; (*b*) A. D. Lynes, J. I. Lovitt, C. Rotella, J. J. Boland, T. Gunnlaugsson and C. S. Hawes, Crystal engineering studies of a series of pyridine-3,5-dicarboxamide ligands possessing alkyl ester arms, and their coordination chemistry, *Results Chem.*, 2022, **4**, 100679; (*c*) S. E. Bodman and S. J. Butler, Advances in anion binding and sensing using luminescent lanthanide complexes, *Chem. Sci.*, 2021, **12**, 2716.

10 (*a*) J. P. Leonard, P. Jensen, T. McCabe, J. E. O'Brien, R. D. Peacock, P. E. Kruger and T. Gunnlaugsson, Self-assembly of chiral luminescent lanthanide coordination bundles, *J. Am. Chem. Soc.*, 2007, **129**, 10986; (*b*) F. Stomeo, C. Lincheneau, J. P. Leonard, J. E. O'Brien, R. D. Peacock, C. P. McCoy and T. Gunnlaugsson, Metal directed synthesis of enatiomerially pure dimetallic lanthanide luminescent triple-stranded helicates, *J. Am. Chem. Soc.*, 2009, **131**, 9636.

11 (*a*) O. Kotova, C. O'Reilly, S. T. Barwich, L. E. Mackenzie, A. D. Lynes, A. J. Savyasachi, M. Ruether, R. Pal, M. E. Möbius and T. Gunnlaugsson, Lanthanide luminescence from supramolecular hydrogels consisting of bioconjugated picolinic-acid-based guanosine quadruplexes, *Chem*, 2022, **8**, 1395; (*b*) T. Gorai, J. I. Lovitt, D. Umadevi, G. McManus and T. Gunnlaugsson, Hierarchical supramolecular co-assembly formation employing multi-component light-harvesting charge transfer interactions giving rise to long-wavelength emitting luminescent microspheres, *Chem. Sci.*, 2022, **13**, 7805.

12 (*a*) T. Tateishi, T. Kojima and S. Hiraoka, Chiral self-sorting process in the self-assembly of homochiral coordination cages from axially chiral ligands, *Commun. Chem.*, 2018, **1**, 18; (*b*) C. Gütz, R. Hovorka, G. Schnakenburg and A. Lützen, Homochiral supramolecular M2L4 cages by high-fidelity self-sorting of chiral ligands, *Chem. – Eur. J.*, 2013, **19**, 10890.

13 (*a*) P. Stachelek, L. MacKenzie, D. Parker and R. Pal, Circularly polarised luminescence laser scanning confocal microscopy to study live cell chiral molecular interactions, *Nat. Commun.*, 2022, **13**, 553; (*b*) A. B. Aletti, S. Blasco, S. J. Aramballi, P. E. Kruger and T. Gunnlaugsson, Sulfate-Templated 2D Anion-Layered Supramolecular Self-Assemblies, *Chem*, 2019, **5**, 2617.

14 (*a*) P. W. Zabierowski, O. Jeannin, T. Fix, J.-F. Guillemoles, L. J. Charbonnière and A. M. Nonat, From ono- to polynuclear coordination complexes with a 2,2′-bipyrimidine-4,4′-dicarboxylate ligand, *Inorg. Chem.*, 2021, **60**, 8304; (*b*) S. Naseri, M. Mirzakhani, C. Besnard, L. Guénée, L. Briant, H. Nozary and C. Piguet, Preorganized polyaromatic soft terdentate hosts for the capture of [Ln(β-diketonate)3] guests in solution, *Chem. – Eur. J.*, 2023, **29**, e202202727; (*c*) D. F. Caffrey, A. J. Savyasachi, K. Byrne, G. Tobin, B. D'agostino, W. Schmitt and T. Gunnlaugsson, Self-assembled bright luminescent hierarchical materials from a tripodal benzoate antenna and heptadentate Eu(III) and Tb(III) cyclen complexes, *Front. Chem. Sci. Eng.*, 2019, **13**, 171.

15 O. Kotova, S. Comby, K. Pandurangan, F. Stomeo, J. E. O'Brien, M. Feeney, R. D. Peacock, C. P. McCoy and

T. Gunnlaugsson, The effect of the linker size in C2-symmetrical chiral ligands on the self-assembly formation of luminescent triple-stranded di-metallic Eu(III) helicates in solution, *Dalton Trans.*, 2018, **47**, 12308.

16 (*a*) D. E. Barry, J. A. Kitchen, L. Mercs, R. D. Peacock, M. Albrecht and T. Gunnlaugsson, Chiral luminescent lanthanide complexes possessing strong (SmIII) circularly polarised luminescence (CPL), and their self-assembly into Langmuir-Blodgett films, *Dalton Trans.*, 2019, **48**, 11317; (*b*) O. Kotova, B. Twamley, J. O'Brien, R. D. Peacock, S. Blasco, J. A. Kitchen, M. Martinez-Calvo and T. Gunnlaugsson, The application of chiroptical spectroscopy (circular dichroism) in quantifying binding events in lanthanide directed synthesis of chiral luminescent self-assembly structures, *Chem. Sci.*, 2015, **6**, 457.

17 (*a*) A. Galanti, O. Kotova, S. Blasco, C. J. Johnson, R. D. Peacock, S. Mills, J. J. Boland, M. Albrecht and T. Gunnlaugsson, Exploring the Effect of Structural Isomerism in Langmuir-Blodgett Films of Chiral Luminescent Eu(III) Self-Assemblies, *Chem. – Eur. J.*, 2016, **22**, 9709; (*b*) J. A. Kitchen, D. E. Barry, L. Mercs, M. Albrecht, R. D. Peacock and T. Gunnlaugsson, Circular polarized lanthanide luminescence from Langmuir-Blodgett films formed from optically active and amphiphilic Eu(III) based self-assembly complexes, *Angew. Chem., Int. Ed.*, 2012, **51**, 704; (*c*) C. Lincheneau, R. D. Peacock and T. Gunnlaugsson, Europium Directed Synthesis of Enantiomerically Pure Dimetallic Luminescent "Squeezed" Triple-Stranded Helicates; Solution Studies, *Chem. – Asian J.*, 2010, **5**, 500.

18 (*a*) D. E. Barry, J. A. Kitchen, K. Pandurangan, A. J. Savyasachi, R. D. Peacock and T. Gunnlaugsson, Formation of enantiomerically pure luminescent triple-stranded dimetallic europium helicates and their corresponding hierarchical self-assembly formation in protic polar solutions, *Inorg. Chem.*, 2020, **59**, 2646; (*b*) J. A. Kitchen, D. E. Barry, L. Mercs, M. Albrecht, R. D. Peacock and T. Gunnlaugsson, Circularly polarized lanthanide luminescence from Langmuir–Blodgett films formed from optically active and amphiphilic EuIII-based self-assembly complexes, *Angew. Chem., Int. Ed.*, 2012, **51**, 704.

19 O. Kotova, J. A. Kitchen, C. Lincheneau, R. D. Peacock and T. Gunnlaugsson, Probing the effects of ligand isomerism in chiral luminescent lanthanide supramolecular self-assemblies; an europium "Trinity Sliotar" study, *Chem. – Eur. J.*, 2013, **19**, 16181.

20 (*a*) I. N. Hegarty, H. L. Dalton, A. F. Henwood, C. S. Hawes and T. Gunnlaugsson, Unexpected linkage isomerism in chiral tetranuclear bis-tridentate (1,2,3-triazol-4-yl)-picolinamide (tzpa) grids, *Chem. Commun.*, 2019, **55**, 9523; (*b*) D. E. Barry, C. S. Hawes, J. P. Byrne, B. la Cour Poulsen, M. Ruether, J. E. O'Brien and T. Gunnlaugsson, A folded [2×2] metallo-supramolecular grid from a bis-tridentate (1,2,3-triazol-4-yl)-picolinamide (tzpa) ligand, *Dalton Trans.*, 2017, **46**, 6464.

21 I. N. Hegarty, H. L. Dalton, A. D. Lynes, B. Haffner, M. E. Möbius, C. S. Hawes and T. Gunnlaugsson, Balancing connectivity with function in silver(I) networks of pyridyltriazole (tzpa) ligands results in the formation of a metallogel, *Dalton Trans.*, 2020, **49**, 7364.

22 (*a*) A. F. Henwood, I. N. Hegarty, E. P. McCarney, J. I. Lovitt, S. Donohoe and T. Gunnlaugsson, Recent advances in the development of the btp motif: A versatile terdentate coordination ligand for applications in supramolecular self-assembly, cation and anion recognition chemistries, *Coord. Chem. Rev.*, 2021, **449**, 214206; (*b*) J. P. Byrne, J. A. Kitchen and T. Gunnlaugsson, The btp [2,6-bis(1,2,3-triazol-4-yl)pyridine] binding motif: a new versatile terdentate ligand for supramolecular and coordination chemistry, *Chem. Soc. Rev.*, 2014, **43**, 5302.

23 (*a*) E. P. McCarney, J. I. Lovitt and T. Gunnlaugsson, Mechanically interlocked chiral self-templated [2]catenanes from 2,6-bis(1,2,3-triazol-4-yl)pyridine (btp) ligands, *Chem. – Eur. J.*, 2021, **27**, 12052; (*b*) C. O'Reilly, S. Blasco, B. Parekh, H. Collins, G. Cooke, T. Gunnlaugsson and J. P. Byrne, Ruthenium-centred btp glycoclusters as inhibitors for Pseudomonas aeruginosa biofilm formation, *RSC Adv.*, 2021, **11**, 16318; (*c*) J. P. Byrne, S. Blasco, A. B. Aletti, G. Hessman and T. Gunnlaugsson, Formation of self-templated 2,6-bis(1,2,3-triazol-4-yl)pyridine [2]catenanes by triazolyl hydrogen bonding: selective anion hosts for phosphate, *Angew. Chem., Int. Ed.*, 2016, **55**, 8938; (*d*) J. P. Byrne, M. Martínez-Calvo, R. D. Peacock and T. Gunnlaugsson, Chiroptical Probing of Lanthanide-Directed Self-Assembly Formation Using btp Ligands Formed in One-Pot Diazo-Transfer/Deprotection Click Reaction from Chiral Amines, *Chem. – Eur. J.*, 2016, **22**, 486.

24 (*a*) W.-L. Chan, C. Xie, W.-S. Lo, J.-C. G. Bünzli, W.-K. Wong and K.-L. Wong, Lanthanide–tetrapyrrole complexes: synthesis, redox chemistry, photophysical properties, and photonic applications, *Chem. Soc. Rev.*, 2021, **50**, 12189; (*b*) S. V. Eliseeva and J.-C. G. Bünzli, Lanthanide luminescence for functional materials and bio-sciences, *Chem. Soc. Rev.*, 2010, **39**, 189.

25 (*a*) D. Parker, J. D. Fradgley and K.-L. Wong, The design of responsive luminescent lanthanide probes and sensors, *Chem. Soc. Rev.*, 2021, **50**, 8193; (*b*) E. M. Surender, S. Comby, B. Cavanagh, O. Brennan, T. C. Lee and T. Gunnlaugsson, Two-photon luminescent bone Imaging using europium nanoagents, *Chem*, 2016, **1**, 438.

26 (*a*) J. P. Byrne, J. A. Kitchen, J. E. O'Brien, R. D. Peacock and T. Gunnlaugsson, Lanthanide Directed Self-Assembly of Highly Luminescent Supramolecular "Peptide" Bundles from α-Amino Acid Functionalized 2,6-Bis(1,2,3-triazol-4-yl) pyridine (btp) Ligands, *Inorg. Chem.*, 2015, **54**, 1426; (*b*) C. S. Bonnet, M. Devocelle and T. Gunnlaugsson, Structural studies in aqueous solution of new binuclear lanthanide luminescent peptide conjugates, *Chem. Commun.*, 2008, 4552.

27 (*a*) S. J. Bradberry, G. Dee, O. Kotova, C. P. McCoy and T. Gunnlaugsson, Luminescent lanthanide (Eu(III)) cross-

linked supramolecular metallo co-polymeric hydrogels: The effect of ligand symmetry, *Chem. Commun.*, 2019, **55**, 1754; (*b*) S. J. Bradberry, J. P. Byrne, C. P. McCoy and T. Gunnlaugsson, Lanthanide luminescent logic gate mimics in soft matter: [H+] and [F-] dual-input device in a polymer gel with potential for selective component release, *Chem. Commun.*, 2015, **51**, 16565.

28 (*a*) W. De, W. Horrocks and D. R. Sudnick, Lanthanide ion probes of structure in biology. Laser-Induced luminescence decay constants provide a direct measure of the number of metal-coordinated water molecules, *J. Am. Chem. Soc.*, 1979, **101**, 334; (*b*) T. J. Sørensen and S. Faulkner, Multimetallic lanthanide complexes: Using kinetic control to define complex multimetallic arrays, *Acc. Chem. Res.*, 2018, **51**, 2493.

29 A. Beeby, I. Clarkson, R. Dickins, S. Faulkner, D. Parker, L. Royle, A. S. de Sousa, J. A. G. Williams and M. Woods, Non-radiative deactivation of the excited states of europium, terbium and ytterbium complexes by proximate energy-matched OH, NH and CH oscillators: an improved luminescence method for establishing solution hydration states, *J. Chem. Soc., Perkin Trans. 2*, 1999, 493.

30 A.-S. Chauvin, F. Gumy, D. Imbert and J.-C. G. Bünzli, Europium and terbium tris(dipicolinates) as secondary standards for quantum yield determination, *Spectrosc. Lett.*, 2004, **37**, 517.

